Passive cooperative targets for subsurface physical and chemical measurements

J.-M Friedt
SENSeOR SAS & FEMTO-ST Institute, Time & Frequency department, Besançon, France
Email: jmfriedt@femto-st.fr

***Abstract*—We investigate the development of passive cooperative targets as sub-surface sensors interrogated by Ground Penetrating RADAR (GPR). Using piezoelectric substrates for converting the incoming electromagnetic pulse to an acoustic wave confined to the sensor surface (Surface Acoustic Wave transducer – SAW) allows for shrinking the sensor dimensions while providing sensing capability through the piezoelectric substrate acoustic wave velocity dependence with the physical quantity under investigation. Two broad ranges of sensing mechanisms are discussed: intrinsic piezoelectric substrate velocity dependence with a quantity – restricted to the measurement of temperature or strain and hence torque or pressure – and extrinsic load dependence on the sensor, allowing for the measurement of variable capacitive or resistive loads. We demonstrate, using readily available surface acoustic wave filters diverted from their original use to become reflective cooperative targets, how commercially available GPR hardware can be used, with minor software addition, to probe such sensors with no hindrance to the shallow subsurface structure detection capability by defining multiple time windows – some for sub-surface monitoring and others for sensing capability.**

***Index Terms*—surface acoustic wave filter, cooperative target, load capacitance, moisture detection**

I. Introduction

Ground Penetrating RADAR is classically used to identify subsurface interfaces detected through the reflection of incoming electromagnetic pulses by dielectric or conductivity mismatch. During such investigations, the time of flight is representative of the depth of the reflector, through the electromagnetic velocity in the medium. In addition to passive interfaces acting as wideband reflectors, some investigations have focused on generating backscattered echoes with characteristics (amplitude, polarization, delay) representative of a physical quantity. For example, [1] considers a buried coaxial wire acting as a delay whose backscattered amplitude is representative of the target orientation. Such considerations are consistent with the broader range of cooperative targets acting as sensors when probed by dedicated hardware – removing the compatibility with available probing equipment – and so-called chip-less RFID (Radio-Frequency IDentifiers) in which the backscattered RADAR cross-section is used for identifying the target.

The context of the present investigation is the monitoring of subsurface soil properties by using passive sensors probed by GPR. In the context of civil engineering applications, such sensors are buried at the time of the construction, in soil or concrete, for future monitoring of the properties of the sensor environment, e.g. temperature, stress or chemical composition of the built structure. Beyond the trivial applications to rebar stress monitoring [2] or concrete temperature assessment [3], monitoring leakage of chemical compounds yielding potential polution of the soil [4] has become mandatory as defined for example in the American Safe Drinking Water Act relased by its Environmental Protection Agency (https://www.epa.gov/ccr).

In this paper, we consider the design of cooperative targets aimed at three purposes:

1) induce a delay which can be uniquely attributed to the sensor and not to clutter (Fig. 1),
2) induce a delay which is representative of a physical quantity to be monitored, with the requirement that no local power source is added to the sensor in order not to limit the sensor life expectancy,
3) prevent the sensing characteristics from reducing the interrogation range by damping the signal.

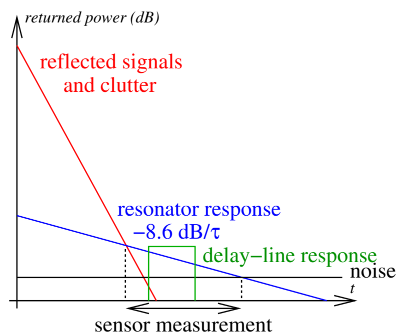

Fig. 1. Time dependence of the various backscattered signal, allowing for time-division multiple access to the radiofrequency channel: a short time window includes the buried interface reflections, while the sensor response is delayed beyond clutter in a longer time-window.

The latter requirement stems from some of the unsuitable approaches in which the transducer antenna is short-circuited by the sensing element. As examples of such poor approaches, [5] proposes adding a hydrogen-sensing layer in parallel to the transduction antenna. Despite some relevant characteristics change dependent on the quantity under investigation, such an approach is doomed to failure in a practical environment since the detection mechanism is associated with signal loss and hence a poor link budget. Similarly, [6] investigates the moisture detection capability of SAW delay lines by loading electrodes acting as reflectors: despite some significant influence of the load capacitance on the sensor response, the associated increased insertion losses significantly reduces the interrogation range over the measurement range. In this paper, we consider acoustically-coupled devices for separating the transduction (converting the incoming electromagnetic wave to an acoustic wave and back when the delayed acoustic wave reaches the electrodes following a travel delay dependent on the environment) from the measurement (loading the reflecting electrodes with a load dependent on the measured quantity) [7].

II. General strategy

A. Sensor signature

Clutter in the initial time window (reflectors the classical GPR user is interested in) might interfere with cooperative target measurement. The sensor design strategy is thus to introduce a signature in the backscattered signal which can be uniquely attributed to the transducer response. In addition, for sensing purposes, it is desirable for the signature to be dependent on one physical quantity and hardly dependent to interfering quantities. One approach lies in introducing a frequency-domain characteristic by using a resonator as co-operative target: the narrowband device stores acoustic energy and slowly releases it with a time constant $Q/(\pi f_0)$ when the excitation pulse stops, with Q the resonator quality factor and f_0 its resonance frequency (Fig. 1, blue). Although used with dedicated measurement electronics not designed for probing sub-surface interfaces, such an approach is not applicable to GPR since the wideband pulse emitted by the instrument does not exhibit spectral characteristics consistent with those of the target. Another approach is to delay the sensor response enough for the backscattered signal to be inconsistent with echoes reflected from passive interfaces (Fig. 1). However, delaying the signal using an electromagnetic delay line would induce an excessively large sensor. It has long been known that storing information in a compact form is achievable by converting the electromagnetic signal to an acoustic signal whose velocity is five orders of magnitude lower – from 300 m/μs for an electromagnetic wave to typically 3000 m/s for acoustic waves. Hence, the sensor dimension is shrunk by the same factor, requiring though clean-room manufacturing capability to fabricate such devices.

However, acoustic transducers are widely used for radiofrequency analog signal processing, especially with the wide availability of wireless communication peripherals. Here, we consider diverting transmission filters as transducers, with one port connected to an external load acting as sensor and the other port acting as communication port with the RADAR system. Such a configuration meets the requirement of separating the transduction and measurement mechanisms and preventing the variable load from degrading the link budget. As such, rather than making a strong difference between delay lines, filters and resonators, we consider such analog radiofrequency signal processing components in a continuity, characterized by different properties (time of flight, or phase, in the former case, resonance frequency in the latter, and somewhat in-between conditions for the filters). These rich classes of designs allow to select the geometry best suited with the interrogating pulse spectra and hence measurement strategy. In this paper, the filter is selected for its impulse response characteristics closely matching the impulse generated by GPR, yet with a longer interaction time of the acoustic wave with the loaded port than in a delay line geometry, yielding enhanced response and lower insertion loss variations as a function of load as will be discussed below.

III. Experimental setup

In order to address a wide audience without dedicated clean-room access, we consider the use of commercially available surface acoustic wave filters rather than designing a dedicated transducer for sensing purposes. The selection criteria, amongst the many available filters, rely on matching the emitted RADAR pulse spectrum, with namely the two characteristics of central frequency and bandwidth. Since GPR antennas are defined by their operating frequency, such a selection should be trivial: however, GPR antennas practically do not operate on a given frequency but on a given wavelength defined by the boundary conditions on the dipole antenna used on the emitter (Fig. 2).

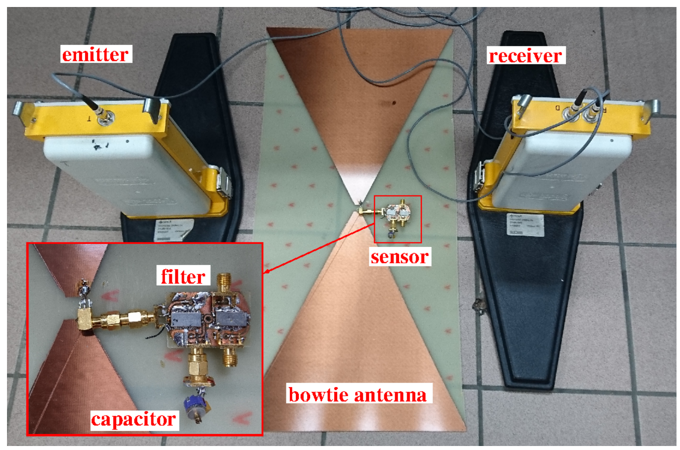

Fig. 2. Experimental setup including a sensor connected to an ultra-wideband antenna operating in the 140-200 MHz range, and the Maå ProEx GPR unit fitted with unshielded 200 MHz antennas.

Since the electromagnetic velocity is dependent on the medium permittivity, the emitted spectrum varies with varying media: matching the filter central frequency with the emitted spectrum is thus environment dependent, and an assessment of the GPR operating frequency must be made in the sensor usage conditions. Similarly, the bandwidth of the filter should be selected to be broad enough for the backscattered pulse to be narrow enough (inversely proportional to the filter bandwidth) to fit the GPR measurement characteristics. Both these quantities are given by the filter manufacturer in their datasheet, but the last characteristic we are interested in, the time delay introduced by the filter, is usually not documented by the manufacturer. Through trial and error, we have selected the TDK/Epcos B3607 (Fig. 3) filter: its center frequency of 140 MHz is compatible with a Malå 200 MHz unshielded dipole antenna located on a concrete slab, and its 6 MHz bandwidth induces a 150 ns returned echo duration, compatible with typical GPR measurement time windows.

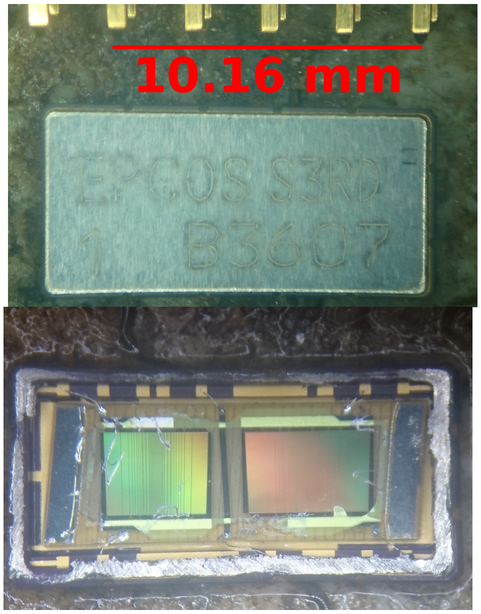

Fig. 3. Pictures of the closed (top) and opened (bottom) SAW filter: despite some scratches made on the electrodes while removing the polymer seal over the electrode area, the general structure of the filter with the input and output interdigitated transducer electrodes is visible.

This particular SAW filter manufacturer provides the filter delay through the group delay entry in the datasheet, documented to be 1.35 μs. However, experimenting with different manufacturers and filter references might yield similar if not better results: in addition to TDK (Japan)/Epcos (Germany), suppliers include Murata (Japan), Fujitsu (Japan), Vectron (Germany), Tai-saw (Taiwan), Triquint (USA) or C-Tech (Korea). As an illustration of such considerations, C-Tech's model 322053 centered on 102.2 MHz, with a bandwidth of 9.86 MHz, insertion losses of 21 dB and a group delay of 3.06$\pm$0.2 μs made of the strongly coupled ($K^2 = 4.5$ %) Y-cut lithium niobate, would meet requirements for a sensor operating with a GPR fitted with 100 MHz antennas.

A. *Measurement*

Having introduced a dedicated signature in the sensor response by delaying its backscattered echoes beyond the latest clutter echo, we need to introduce some signature as to the measured physical quantity to convert a tag into a sensor. Two approaches are well known: exploiting intrinsic material property dependence with the environment, and adding an external load to the transducer. The intrinsic material property dependence with the environment requires, for the anisotropic material piezoelectric substrates are made of, dedicated modelling tool including, for an accurate behavior understanding, the electrodes patterned over the piezoelectric substrate. The physical quantities accessible this way are temperature, stress and thus pressure, and chemical binding by varying boundary conditions of the acoustic wave confined to the substrate surface [8], [9], [10] The latter approach, a variable load attached to one port of the transducer while the second port is used for radiofrequency transduction, will be the one of interest to us. Indeed, in this particular investigation, observing moisture content in soil is best achieved by monitoring capacitance change between two electrodes surrounded by the medium under investigation. Since the capacitance of this setup rises proportionally with the relative permittivity, and water induces a huge permittivity variation – from $\varepsilon_r \simeq 5$ for dry sand to $\varepsilon_r = 30$ for wet sand [11] and even $\varepsilon_r = 80$ for fresh water, the ten-fold variation of capacitance is considered as the quantity to be investigated. The influence of the variable load connected to one port of the filter on the other port of the filter is discussed in [12], where the maximum influence is shown to be induced by a load impedance equal to the inverse of the filter port admittance. Furthermore, the effect of the load on the short-circuit response is magnified by the piezoelectric electromechanical coupling coefficient: strongly coupled materials, with which broadband radiofrequency filters are often made of, will induce larger effects than weakly coupled materials. If the load is purely capacitive and the filter is resistive in its bandpass, then an impedance matching circuit must be added to induce a significant effect on the transduction port: in our case, a fixed inductance is added in series with the capacitance to bring the phase close to zero at a frequency within the emitted GPR pulse and hence within the bandpass of the filter acting as a sensor (Fig. 4).

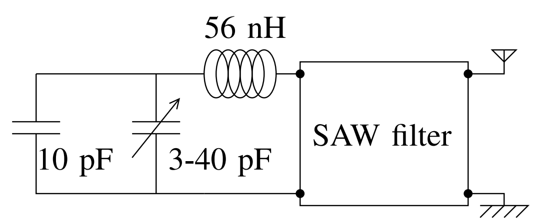

Fig. 4. Coupled acoustic transducer with a load tuned to the operating frequency.

IV. Experimental results

The filter is used in reflection mode, with the S_{11} measurement representative of the load impedance through acoustic coupling of both ports. Fig. 5 exhibits the reflection coefficient measurements in the time domain, extracted as the inverse Fourier transform of the frequency domain characteristics measured by a network analyzer. The two main features are on the top chart the two echoes with time delays of 2.7 μs (two-way trip) and, since the ports are not matched with the transducer impedance, the four-way trip at 5.4 μs, with the latter significantly attenuated and hardly usable for wireless measurement purposes. On the bottom chart, the phase evolution with load capacitance exhibits a large variation by over 140° for load capacitances ranging from 14 to 63 pF. Working on the phase rather than on the amplitude, as considered by [1], is desirable since the amplitude is strongly dependent on other factors than target properties, including the medium through which the RADAR pulse propagates. On the other hand, the phase is solely dependent on the distance from the RADAR to the target, and considering a differential approach in which multiple reflectors are located on the sensor acoustic path, the RADAR to target distance dependence can be eliminated by computing the phase difference between reflected echoes.

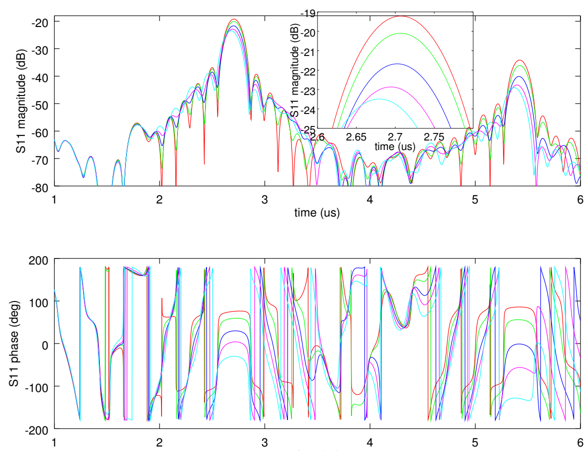

Fig. 5. Magnitude (top) and phase (bottom) of the time-domain response of the filter used in reflection mode and loaded with a variable capacitance in parallel to a fixed 10 pF capacitance. The sum of the capacitances is respectively 14 pF, 26 pF, 38 pF, 51 pF, 63 pF for the red, green, blue, magenta and cyan curves. Inset: zoom on the magnitude of the first echo, emphasizing the losses confined to the 19 to 24 dB range over the whole capacitance range.

The actual load capacitance value was computed by measuring the resonance frequency $\frac{1}{2\pi}\sqrt{\frac{1}{LC}}$ of the LC tank using a broadband network analyzer operating in the 50-200 MHz range, with $L = 56$ nH fixed and resonance frequencies ranging from 85 to 180 MHz. The second backscattered echo is characterized by twice the losses – since the acoustic pulse travelled twice through the acoustic cavity – but also twice the phase rotation. The most significant characteristic of this calibration curve is on the one hand the significant phase rotation induced by varying the load capacitance, but most significantly the low acoustic losses induced by the varying load. Indeed, loosing the returned signal when the measurement is occurring because the backscatter efficiency is lost for some range of the measured quantity is of little use in a practical application.

Prior to measuring the sensor with a (pulsed RADAR) GPR unit, the characterization of the sensor is performed in the frequency domain using a network analyzer. One signal processing subtlety worth mentioning when converting the frequency domain characterization of a delay line to the time domain is the fact that the central frequency lies half-way in the dataset, while the Fourier transform convention in Matlab or GNU/Octave is that the 0-frequency (DC offset) and sampling frequency lie at the extremes of the dataset (beginning and end of the dataset). Hence, converting the frequency-domain characteristics of the delay line to a time-domain characteristics requires, to reach a baseband in which the central frequency has been eliminated, to swap the first and the second half of the dataset, an operation performed by the `fftshift` operator in both languages. Thus, the $s_{11} \in \mathbb{C}$ reflection coefficient is converted from frequency domain to time domain with `ifft(fftshift(`s_{11}`))` with a time axis spanning from 0 to the number of samples times the sampling time step, and a time step given by the inverse of the frequency span. This processing procedure has been verified to be consistent with the Time-Domain (TDR) option of a Rohde & Schwartz ZVB network analyzer.

V. Measurement distance assessment

One issue with extrinsic load variation is the reflected power dependence with the load. Indeed, if the returned power significantly varies within the load measurement range, then either the interrogation range is reduced, or the measurement distance must be restricted. Separating the measurement (load) port from the transduction port already allows for a rationale approach to sensor design. As can be seen in [5], loading the antenna with the sensing layer conductive variation induces a drop in the S_{11} which will necessarily translate in a loss of measurement range since the impedance matching conditions between the antenna and the transducer will no longer be met. Even decoupling the transduction port and the measurement port might yield significant returned power variation: in [6], the relative losses between adjacent echoes vary by up to 20 dB. Since the RADAR equation states that the returned power varies as the fourth power of distance, varying the backscattered signal (equivalent to the target cross section in the RADAR equation) by 20 dB induces a range drop by a factor of $10^{20/40} \simeq 3$. In our case, the backscattered signal only varies by 5 dB, inducing a measurement distance loss of 1.3 with respect to the best link budget condition.

Considering the 19 to 25 dB losses, depending on the load capacitance, of the backscattered signal, the measurement distance is estimated from the dynamic range of the GPR. Assuming a $\eta = 100$ dB dynamic range between emitter and receiver, unit gain antennas and perfect impedance matching, then the free-space path loss (FSPL) and backscattering efficiency (IL) will induce an estimate of the measurement distance d of

$$\eta = FSPL + IL = 40\log_{10}(d) + 40\log_{10}(f) - 147.55 \times 2$$

when working at frequency $f = 140$ MHz, where $-147.55 = 20\log_{10}(4\pi/c)$ provides the conversion factor between frequency and wavelength through the electromagnetic velocity c in addition to energy spreading over a 4π steradian sphere with the target acting as a point-like source. Numerical application with $IL \in [19; 25]$ dB induces $d = 10^{(\eta-40\log_{10}(f)+147.55\times2-IL)/40}$ which yields, after numerical application to estimate the upper limit on the interrogation distance, to $d \in [13; 18]$ m. Such measurement distances are well within the classical measurement distances of GPR in temperate climates, making the cooperative target an ideal complement to passive sub-surface interface monitoring. However, since no conduction losses have been included in this estimate. the 13 m measurement distance is an upper bound relevant to purely dielectric materials with no imaginary part to the permittivity.

VI. Software for Sensor Probing

Most commercial GPR (Fig. 2) architectures are based on a stroboscopic sampling approach, a tradeoff between sampling rate, analog-to-digital converter resolution, and computational power needed to acquire the time domain response of the sub-surface reflectors. The drawback of a stroboscopic measurement is that N samples require N pulse emissions and waiting for all returned echoes to fade out before a new pulse is emitted (Fig. 6). The advantage of the stroboscopic measurement for sensor probing is that all recorded samples are independent from each other, with a time delay between emitted pulse and track-and-hold locking defined by software. Hence, separate measurement time windows are easily implemented by sweeping the time delay between the emitted pulse and the track-and-hold sampling time first with small values for shallow interface monitoring, and then with larger values for sensor measurement at time delays beyond clutter (Fig. 7).

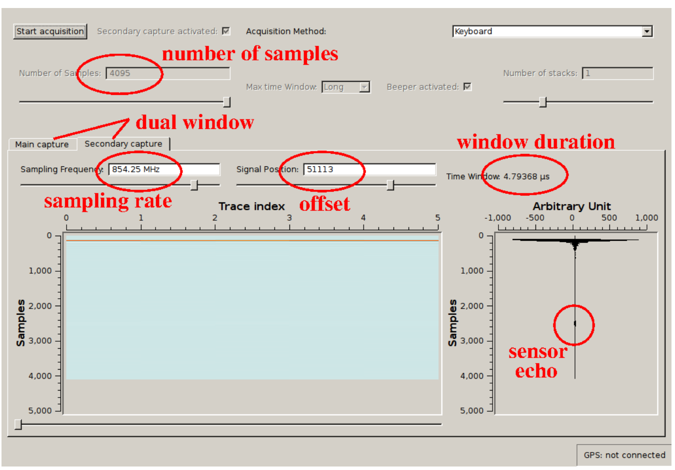

Fig. 6. Graphical user interface used in a classical mode in which one continuous window probes the echoes for a duration long enough to include the sensor response. In this configuration, the sampling rate must be decreased and thus the shallow interface depth measurement is degraded. The GPR is here fitted with 100 MHz unshielded antennas, and a slow sampling rate of 854 MHz is needed to probe a window duration long enough to include the sensor response.

The Malå ProEx GPR default software does not allow such features. However, the ethernet communication protocol is trivially reverse engineered to allow for a custom implementation with the features required for sensing purposes. Such a software is made available to the interested audience at https://sourceforge.net/projects/proexgprcontrol/. A single sampling frequency is common to both time windows, a shallow feature measurement capability as classically needed for GPR measurements, and a deep measurement beyond buried interface detection capability in which the buried sensor is the only possible backscattered signal source. Hence, the signal to noise ratio and hence detection capability is excellent thanks to the lack of clutter in the latter time window.

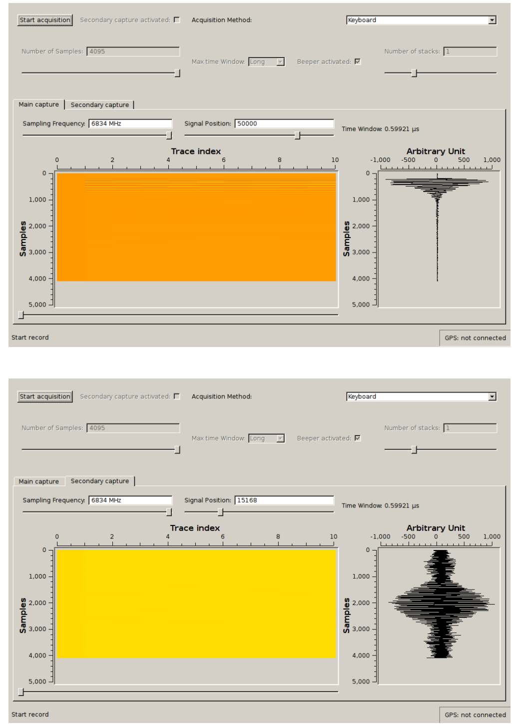

Fig. 7. Graphical user interface: top the shallow interface window, bottom the window tracking the sensor response. Since the two windows are separate, a fast sampling rate is used to accurately detect the shallow interfaces, and the time gap between the shallow interface backscattered signals and the delayed sensor echo is not sampled. The GPR is here fitted with 200 MHz unshielded antennas. Notice that both time windows sample at a fast sampling rate, but the time offset is adapted to include either the emitted pulse, or the echo returned from the sensor.

Notice that the GPR pulses are broadband enough that the 140 MHz filter response is acquired whether 100 MHz or 200 MHz unshielded antennas are used. However, the returned power is dependent on the overlap of the emission spectra with the sensor transfer function: using antennas not matching the transfer function of the sensor will lower the interrogation range but will not prevent the actual measurement. Such considerations are representative of those met when the emitted pulse central frequency varies as the permittivity of the soil the GPR antennas are located on varies.

VII. Measurement Results

The (antenna connected) input port and the (load connected) output port are coupled through the acoustic wave traveling between both electrode sets. We have demonstrated previously that varying the load impedance changes the phase of the signal seen from the communication port. However, when connecting the communication port to an antenna, the impedance is all but constant as a 50 Ω resistive load. The load impedance range becomes dependent on the antenna impedance: despite impedance matching, the capacitance range that exhibited the best response when monitored on a network analyzer did not yield significant phase shift in a remote measurement process through the GPR signal. Nevertheless, the acoustic wave propagating on a lithium niobate substrate exhibits strong velocity dependence with temperature, and monitoring the phase of the signal at the frequency at which the maximum of the power is returned (as observed on the Fourier transform of the echo) displays a strong correlation with temperature. In Fig. 8, we demonstrate the remote measurement, through a GPR measurement, of the SAW filter temperature. The bottom chart is obtained after removal of a linear fit of the slow phase drift, and exhibits the two sharp phase changes as the filter is heated with a soldering iron and then cooled with a freezing gas flow.

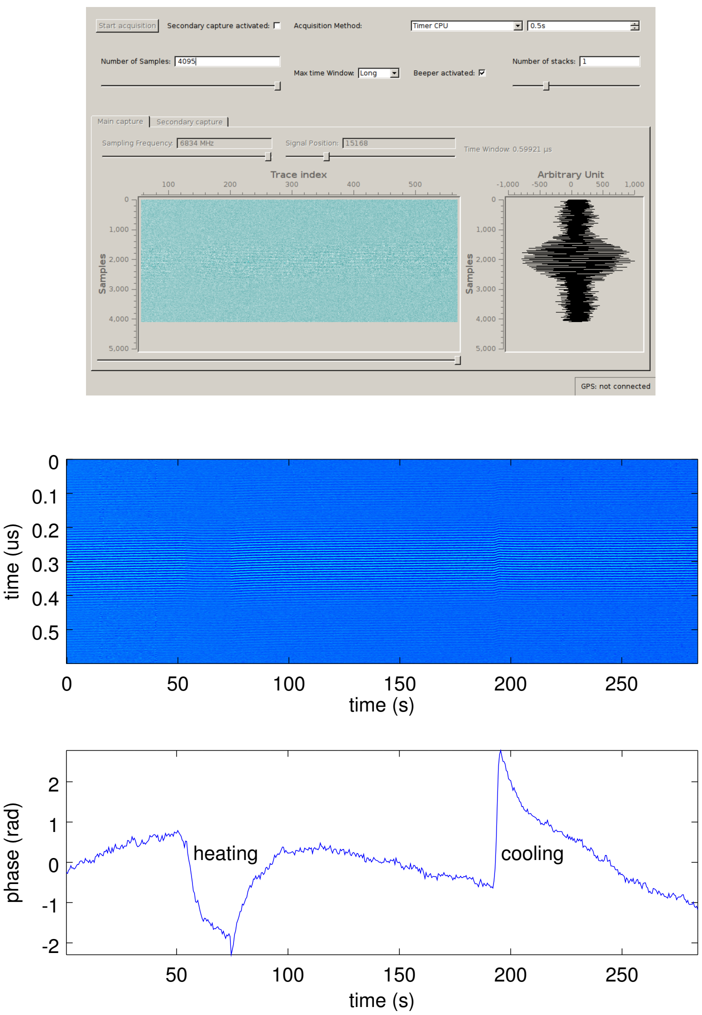

Fig. 8. Top: graphical user interface focusing on the SAW filter signal. Bottom: phase of the maximum of the Fourier transform of the echo, representative of the acoustic velocity dependence with temperature. In the top chart, the vertical (fast axis) time scale is referred to 0 μs despite a 2.7 μs offset introduced during the recording.

We here reach the limits of diverting a radiofrequency SAW filter for sensing purposes as a cooperative target to GPR: a differential measurement with multiple echoes returned by the sensor to get rid of distance and drift dependence is mandatory, in addition to an acoustic coupling between communication and load ports specifically designed for sensing purposes [13].

VIII. Conclusion

We have demonstrated the use of general purpose radiofrequency filters based on surface acoustic wave propagation as transducers acting as cooperative targets to Ground Penetrating RADAR for sensing purposes. The use of a transponder separating the transduction principle from the measurement principle through a variable impedance load provides low backscattered signal losses with a significant phase rotation allowing to keep an acceptable link budget mostly independent of the quantity under measurement. A variable capacitance was used to demonstrate the operating principle for a continuously varying load, representative of operating conditions of a moisture detector.

Acknowledgment

The Malå ProEx GPR control unit acquisition was funded by a grant from the Franche-Comté district. Fruitful discussions with G. Audouin (Total), S. Ballandras and T. Laroche (Frec'n'sys, Besançon, France) helped improve the layout of this document.

References

[1] C. Allen, K. Shi, and R. Plumb, "The use of ground-penetrating radar with a cooperative target," *IEEE Transactions on Geoscience and Remote Sensing*, vol. 36, no. 5, pp. 1821–1825, 1998.

[2] B. Han, Y. Wang, S. Dong, L. Zhang, S. Ding, X. Yu, and J. Ou, "Smart concretes and structures: A review," *Journal of Intelligent Material Systems and Structures*, vol. 26, pp. 1303–1345, July 1 2015.

[3] A. Norrisa, M. Saafib, and P. Rominec, "Temperature and moisture monitoring in concrete structures using embedded nanotechnology/microelectromechanical systems (mems) sensors," *Construction and Building Materials*, vol. 22, no. 2, pp. 111–120, February 2008.

[4] F. Bender, R. Mohler, A. Ricco, and F. Josse, "Identification and quantification of aqueous aromatic hydrocarbons using SH-surface acoustic wave sensors," *Anal. Chem*, vol. 86, no. 3, pp. 1794–1799, 2014.

[5] J. Lee, J. Oh, J. Jun, and J. Jang, "Wireless hydrogen smart sensor based on Pt/graphene-immobilized radio-frequency identification tag," *ACS nano*, vol. 9, no. 8, pp. 7783–7790, 2015.

[6] L. Reindl, C. Ruppel, A. Kirmayr, N. Stockhausen, M. Hilhorst, and J. Balendonck, "Radio-requestable passive SAW water-content sensor," *IEEE Transactions on Microwave Theory and Techniques*, vol. 49, no. 4, pp. 803–808, 2001.

[7] J.-M. Friedt and A. Hugeat, "A low cost approach to acoustic filters acting as GPR cooperative targets for passive sensing," in *Advanced Ground Penetrating Radar (IWAGPR), 2015 8th International Workshop on*. IEEE, 2015, pp. 1–4.

[8] H.-K. Oh, W. Wang, K. Lee, C. Min, and S. Yang, "The development of a wireless love wave biosensor on 41° YX $LiNbO_3$," *Smart Mater. Struct.*, vol. 18, p. 025008, 2009.

[9] T. Song, S. Y. Song, H. Yoon, and K. Lee, "Development of a wireless love wave biosensor platform for multi-functional detection," *Jpn. J. Appl. Phys.*, vol. 50, p. 06GL09, 2011.

[10] F. Bender, F. Josse, R. Mohler, and A. Ricco, "Design of SH-surface acoustic wave sensors for detection of ppb concentrations of BTEX in water," in *2013 Joint UFFC, EFTF and PFM Symposium*, 2013, pp. 628–631.

[11] J.-L. Davis and A. Annan, "Ground penetrating radar for high resolution mapping of soil and rock stratigraphy," *Geophysical prospecting*, vol. 37, pp. 531–551, 1989.

[12] E. Mackensen and L. Reindl, "Wireless passive SAW identification marks and sensors," in *Smart Sensors and MEMS*. Springer, 2004, pp. 155–202.

[13] J.-M. Friedt, A. Saintenoy, S. Chrétien, T. Baron, E. Lebrasseur, T. Laroche, S. Ballandras, and M. Griselin, "High-overtone bulk acoustic resonator as passive ground penetrating RADAR cooperative targets," *Journal of Applied Physics*, vol. 113, no. 13, p. 134904, 2013.